BILINGUAL PUBLISHING GROUP

Journal of Environmental & Earth Sciences
https://journals.bilpubgroup.com/index.php/jees

ARTICLE

Study on the Characteristics of High-Frequency Electromagnetic Wave Detection in Goaf Areas along Coal Seam Boreholes

Maolin Yang

UCHN Energy Investment Group, SHEN DONG COAL Geological Survey Company, Ordos 017000, China

ABSTRACT

China has a long history of coal mining, among which open-pit coal mines have a large number of small coal mine goafs underground. The distribution, shape, structure and other characteristics of goafs are isolated and discontinuous, and there is no definite geological law to follow, which seriously threatens the safety of coal mine production and personnel life. Conventional ground geophysical methods have low accuracy in detecting goaf areas affected by mechanical interference from open-pit mines, especially for waterless goaf areas, which cannot be detected by existing methods. This article proposes the use of high-frequency electromagnetic waves for goaf detection. The feasibility of using drilling radar to detect goaf was theoretically analyzed, and a goaf detection model was established. The response characteristics of different fillers in the goaf under different frequencies of high-frequency electromagnetic waves were simulated and analyzed. In a certain open-pit mine in Inner Mongolia, 100MHz high-frequency electromagnetic waves were used to detect the goaf through directional drilling on the ground. After detection, excavation verification was carried out, and the location of one goaf detected was verified. The results of engineering practice show that the application of high-frequency electromagnetic waves in goaf detection expands the detection radius of boreholes, has the advantages of high efficiency and accuracy, and has important theoretical and practical significance.

Keywords: Underground Coal Mine; Goaf; High-Frequency Electromagnetic Wave (HFEW); Borehole

*CORRESPONDING AUTHOR:

Maolin Yang, UCHN Energy Investment Group, SHEN DONG COAL Geological Survey Company, Ordos 017000, China; Email: 10030623@ceic.com

ARTICLE INFO

Received: 12 May 2025 | Revised: 26 May 2025 | Accepted: 29 May 2025 | Published Online: 8 July 2025
DOI: https://doi.org/10.30564/jees.v7i7.9977

CITATION

Yang, M., 2025. Study on the Characteristics of High-Frequency Electromagnetic Wave Detection in Goaf Areas along Coal Seam Boreholes. Journal of Environmental & Earth Sciences. 7(7): 272–284. DOI: https://doi.org/10.30564/jees.v7i7.9977

COPYRIGHT

Copyright © 2025 by the author(s). Published by Bilingual Publishing Group. This is an open access article under the Creative Commons Attribution-NonCommercial 4.0 International (CC BY-NC 4.0) License (https://creativecommons.org/licenses/by-nc/4.0/).

1. Introduction

China's coal mining industry, a cornerstone of its energy infrastructure, has operated for decades, leaving behind vast underground voids known as goafs. These abandoned spaces, formed after coal extraction, are often poorly mapped and unstable, posing catastrophic risks such as ground subsidence, gas explosions, and structural collapses. Recent studies estimate that over 30% of China's active coal mines are situated above legacy goafs, with incidents like the 2019 Shanxi goaf collapse causing fatalities and economic losses exceeding $50 million [1,2]. The urgency to address these hazards has intensified as mining depths exceed 1,000 meters, exacerbating geological uncertainties. Traditional goaf detection methods, while foundational, struggle to meet the precision and adaptability demands of modern mining.

1) Seismic Exploration: a cornerstone of subsurface imaging, operates on the principle of analyzing reflected or refracted elastic waves generated by controlled sources (e.g., explosives or vibroseis trucks) [3]. When seismic waves encounter interfaces between materials of differing acoustic impedances-such as the boundary between intact coal and an air-filled goaf-a portion of the energy reflects back to the surface, where geophones record travel times and amplitudes. Advanced processing algorithms, including pre-stack depth migration, convert these signals into 2D/3D structural maps. In the Ordos Basin, seismic surveys have successfully imaged large-scale faults and stratigraphic discontinuities at depths up to 800 meters, achieving lateral resolutions of 10–20 meters [4]. However, the method's effectiveness diminishes sharply for small-scale goafs (<8 meters) due to the inherent wavelength limitations of low-frequency seismic waves (typically 10–50 Hz). For instance, a 2018 survey in the Huainan coalfield failed to detect a 6-meter-wide goaf, leading to unanticipated roof collapse during subsequent longwall mining [5]. Additional drawbacks include exorbitant costs (averaging $800,000 per survey), vulnerability to ambient vibrations from mining machinery, and the reliance on specialized interpreters—a resource often scarce in remote mining regions. These limitations underscore seismic exploration's inadequacy for precision goaf detection in modern deep-mining contexts.

2) Magnetic Exploration: Magnetic exploration exploits variations in the Earth's magnetic field caused by contrasts in rock magnetization, particularly in iron-rich formations [6]. In coal mines where goaf boundaries are associated with collapsed roofs containing magnetite debris, this method measures magnetic anomalies to map void edges. For example, in the Shuozhou coalfield, magnetic surveys achieved 85% accuracy in delineating goafs within magnetically homogeneous strata, with anomalies ranging from 50 to 200 nT [7]. However, the technique's utility collapses in non-magnetic environments, such as lignite deposits in Yunnan, where goafs lack ferromagnetic signatures. Surface interference from power lines, rail tracks, and machinery further complicates data interpretation, generating false positives that mimic goaf signals. A 2021 study in the Hebei province revealed that 30% of magnetic anomalies initially classified as goafs were later attributed to buried pipelines and industrial waste [8]. Consequently, magnetic exploration remains niche, applicable only to specific geological settings with minimal anthropogenic disturbances.

3) Low-Frequency Electromagnetic Exploration: Low-frequency EM methods (1–10 kHz) infer subsurface conductivity by transmitting electromagnetic pulses and measuring their attenuation and phase shifts [9–12]. Water-saturated goafs, with conductivity values 10–100 times higher than coal, produce distinct EM anomalies. Field trials in the flooded Fuxin mines demonstrated 70% detection accuracy for water-filled voids at depths up to 80 meters . However, the method falters in dry or debris-filled goafs, where conductivity contrasts are negligible. Depth penetration is another critical constraint: at 150 meters, signal strength attenuates by over 95%, rendering the technique ineffective for deep mining applications. Furthermore, surface EM noise from power grids and communication systems introduces artifacts that mimic goaf responses. [13]. These limitations restrict low-frequency EM to shallow, water-dominated environments—a shrinking subset as mining progresses into deeper, drier strata.

4) High-Density Resistivity Method: The high-density resistivity method maps subsurface resistivity variations by injecting electrical currents through surface electrode arrays and measuring potential differences [14]. Air-filled goafs, with near-infinite resistivity contrasts against coal, generate detectable anomalies. In the arid Shendong coalfield, this technique achieved 65% detection accuracy for

voids larger than 5 meters [15]. Additionally, the method's detection depth rarely exceeds 50 meters in conductive media, and its spatial resolution degrades rapidly with depth. These issues relegate high-density resistivity to a supplementary role in goaf detection workflows.

5) Borehole Logging: Borehole logging employs downhole tools—such as density, neutron, and resistivity sondes-to measure physical rock properties within drilled holes [16]. In the Xinjiang coalfield, density logs identified localized fractures within 2 meters of boreholes, achieving millimeter-scale vertical resolution . However, the method's lateral detection radius is limited to <2 meters, necessitating dense drilling grids for comprehensive coverage-a prohibitively expensive approach in deep mines. Moreover, logging cannot directly detect goafs beyond the borehole wall or characterize filler materials. While invaluable for calibrating seismic or EM models, standalone applications are impractical. A 2019 project in Anhui province required 120 boreholes to map a 1 km² goaf zone—a stark contrast to the efficiency demands of modern mining [17].

6) Gravity Exploration: Gravity surveys detect subsurface density contrasts by measuring minute variations in gravitational acceleration (precision: 0.01 mGal) [18]. The method's resolution is insufficient for voids <50 meters, and high-precision gravimeters are cost-prohibitive for routine use. Furthermore, gravity anomalies cannot differentiate between goafs and other low-density features like sedimentary basins or fault zones. These constraints limit gravity exploration to regional-scale studies rather than targeted goaf detection.

7) Ground-Penetrating Radar (GPR): GPR profiles shallow subsurface structures (typically <30 meters) by transmitting high-frequency electromagnetic pulses (100–1,000 MHz) and analyzing reflections [19,20]. In the dry, shallow coal seams of Shaanxi, GPR achieved 5-centimeter resolution, delineating goaf boundaries with 90% accuracy. However, signal attenuation in conductive media-such as water-saturated strata or clay-rich roofs—reduces effective depth to <10 meters. Antenna size further complicates deployment in narrow underground roadways, where space constraints prevent optimal positioning.These shortcomings restrict GPR to niche applications in shallow, dry environments.The same problem also exists for cross hole electromagnetic wave CT detection [21] and borehole radar [22,23] of goaf.

In summary, existing geophysical methods for goaf detection face critical limitations: seismic exploration, transient electromagnetic techniques, and magnetic prospecting struggle to delineate precise goaf boundaries; high-density resistivity and ground-penetrating radar (GPR) exhibit restricted detection depths; while borehole logging and gravity exploration lack direct applicability for goaf identification. Furthermore, escalating mining scales and depths exacerbate challenges, including complex geological conditions, heterogeneous fill materials, and pervasive environmental interference, which collectively undermine detection accuracy. To address these constraints, this study proposes a novel high-frequency electromagnetic wave-based borehole detection method. By deploying radial scanning within boreholes, this approach aims to enhance the precision of goaf identification in proximal coal seams, thereby advancing safety and efficiency in coal mine production.

This study develops a numerical simulation model for goaf detection, systematically investigating the response characteristics of high-frequency electromagnetic waves to coal seam goafs with varying frequency, filling materials and borehole trajectory. By integrating field data from underground engineering practices in Shanxi coal mines, the research validates the method's effectiveness in real-world scenarios. The findings establish a robust theoretical foundation for high-frequency electromagnetic wave-based goaf detection, offering actionable insights to enhance mining safety and operational precision.

2. Principle of HFEW Detection

According to the theory of electromagnetic wave propagation, high-frequency electromagnetic waves propagate in a medium according to Maxwell's equations. The Maxwell equation system indicates that a changing electric field generates a changing magnetic field, which in turn triggers a changing electric field. The electric and magnetic fields are converted into each other and propagate at a finite speed towards a distance, forming electromagnetic waves. The wave equation of electromagnetic waves is as follows:

$$\nabla^2 \vec{\mathrm{E}} = \mu\sigma\frac{\partial \vec{\mathrm{E}}}{\partial \mathrm{t}} + \mu\sigma\frac{\partial^2 \vec{\mathrm{E}}}{\partial \mathrm{t}^2} \quad (1)$$

$$\nabla^2 \vec{H} = \mu\sigma\frac{\partial \vec{H}}{\partial t} + \mu\sigma\frac{\partial^2 \vec{H}}{\partial t^2} \quad (2)$$

where $\vec{H}$ is r magnetic field strength, unit: A/m; $\vec{E}$ is the electric field strength, unit V/m; σ is conductivity, unit: S/m; ε is the dielectric constant, unit: F/m; μ is magnetic permeability, unit: H/m. Generally, $\vec{E}$ and $\vec{H}$ can be with three components, and each component is a function of a three-dimensional coordinate variable (x, y, z) and time *t*.

When high-frequency electromagnetic waves are detected in boreholes, the geological conditions are complex, and the strata belong to lossy media. Electromagnetic waves have propagation losses during the propagation process, and the energy of electromagnetic waves decreases with increasing propagation depth. In a conductive medium, the constant of attenuation per unit distance during the propagation of planar electromagnetic waves is called the attenuation constant, and the phase lagged behind per unit distance is called the phase constant. The attenuation constant and phase constant are related to the properties of the medium and electromagnetic waves, and the relationship is as follows:

$$\alpha = \sqrt{\frac{\mu\varepsilon}{2}\left[\sqrt{1+\left(\frac{\sigma}{\omega\varepsilon}\right)^2}-1\right]} \quad (3)$$

$$\beta = \omega\sqrt{\frac{\mu\varepsilon}{2}\left[\sqrt{1+\left(\frac{\sigma}{\omega\varepsilon}\right)^2}+1\right]} \quad (4)$$

In equations (3) and (4), α is the attenuation constant, expressed in Nb/m; β is the phase constant, measured in rad/m; σ is conductivity, unit S/m; ε is the dielectric constant, measured in F/m; μ is magnetic permeability, unit H/m; ω is the angular frequency of electromagnetic waves, measured in rad/s.

Equations (1) and (2) replace the dielectric constant ε with a complex dielectric constant ε_c in a conductive medium, and the solution to the one-dimensional wave equation of a plane wave propagating along the z-axis direction is:

$$E_x(z) = E_0 e^{-(\alpha+i\beta)z} \quad (5)$$

$$H_y(z) = \frac{1}{Z_c}E_0 e^{-(\alpha+i\beta)z} \quad (6)$$

where Ex (z) and Hy (z) represent the electric field strength and magnetic field strength of electromagnetic waves propagating along the z-axis, respectively, and α is the attenuation constant in Nb/m; β is the phase constant in rad/m.

According to equations (3) to (6), it can be seen that the amplitude of electric field strength and magnetic field strength decays as $e^{-\alpha z}$. The conductivity has a significant impact on the energy attenuation of high-frequency electromagnetic waves, and the higher the conductivity, the greater the attenuation. That is to say, the higher the resistivity, the smaller the attenuation. The electrical resistivity of coal seams is generally high, so high-frequency electromagnetic waves have the ability to penetrate coal seams, and can be detected in coal seams using borehole radar.

Electromagnetic waves will reflect and refract when they encounter different media interfaces during propagation. The propagation directions of incident waves, reflected waves, and refracted waves of electromagnetic waves satisfy the laws of reflection and refraction. The distance between the transmitting antenna and the receiving antenna of the borehole radar is small. The reflection coefficient R12 and refractive index T12 at the interface from the first layer of medium 1 to the second layer of medium 2 are:

$$R_{12} = \frac{1-\sqrt{\frac{\varepsilon_2}{\varepsilon_1}}}{1+\sqrt{\frac{\varepsilon_2}{\varepsilon_1}}} = \frac{\sqrt{\varepsilon_1}-\sqrt{\varepsilon_2}}{\sqrt{\varepsilon_1}+\sqrt{\varepsilon_2}} \quad (7)$$

$$T_{12} = \frac{2}{1+\sqrt{\frac{\varepsilon_2}{\varepsilon_1}}} = \frac{2\sqrt{\varepsilon_1}}{\sqrt{\varepsilon_1}+\sqrt{\varepsilon_2}} \quad (8)$$

where $\varepsilon_1, \varepsilon_2$ are the dielectric constants of medium 1 and medium 2, respectively.

The greater the difference in dielectric constant between medium 1 and medium 2, the higher the reflection coefficient and the stronger the reflection, which is more conducive to drilling radar detection. When the dielectric constants of medium 1 and medium 2 are the same, the reflection coefficient is 0, and no reflection occurs, only refraction (i.e., transmission) occurs.

The dielectric constant of coal seams is related to the degree of coal metamorphism, water, temperature, and mineral content, generally distributed between 2 and 5. When the goaf is filled with water, the dielectric constant of water is relatively large, generally greater than 50. When the goaf is filled with air, the dielectric constant of air is 1. Therefore, when the goaf is filled with water or gas, it can form a reflective interface with the coal. When the high-frequency electromagnetic waves emitted by the drilling radar propagate in the coal seam, they will be reflected at the interface formed between the goaf and the coal. The reflected electromagnetic waves can be received

by the receiving antenna. By analyzing the characteristics of the reflected waves, the position and characteristics of the goaf can be analyzed.

3. Theoretical Characteristics Analysis of HFEW Detection of Goaf

In order to better understand the characteristics of using HFEW to detect goaf in boreholes, a numerical simulation analysis model is established to analyze the response characteristics of HFEW detection under different HFEW frequencies and filling materials in goaf. This chapter first introduces the basic principles of HFEW simulation, then describes the established model, and finally conducts characteristics analysis for HEW detection.

3.1. Numerical Simulation Principle of HFEW

At present, there are three kinds of electromagnetic wave numerical simulation methods: ray tracing method, finite difference time domain (FDTD) method and finite element method [24]. Gprmax is an open source FDTD based GPR forward simulation software developed by Edinburgh University [25,26].

FDTD divides the simulation space into finite spatial grids (**Figure 1**). The electromagnetic field of each grid can be determined by six components of Ex, Ey, Ez, Hx, Hy and Hz, and then the Maxwell equation in time domain can be directly solved by finite difference.

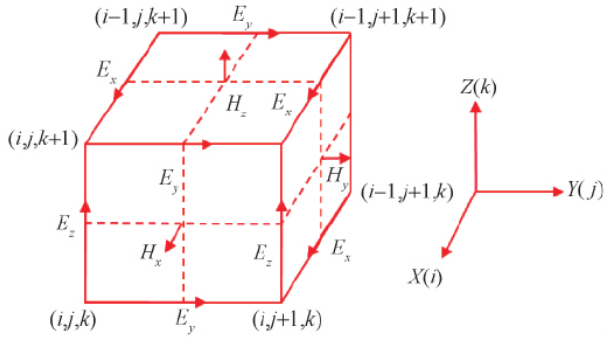

Figure 1. FDTD Method Difference Grid.

After the initial conditions and boundary conditions of the field are given, the distribution values of the spatial electromagnetic field at each time are obtained in turn, that is, the simulation results of the electromagnetic field in the simulation space area are obtained.

Gprmax is an open-source electromagnetic wave simulation software based on the Finite-Difference Time-Domain (FDTD) method, specifically designed for Ground Penetrating Radar (GPR) and other electromagnetic applications. Developed by the University of Edinburgh in the UK, it is widely used in geological exploration, civil engineering, archaeology, snow and ice layer research, and underground target detection. Users can simulate the propagation, reflection, and scattering processes of electromagnetic waves in different media by customizing geometric models, material properties, and excitation signals, thereby predicting radar signal responses and optimizing detection strategies.

The Gprmax software supports complex 3D modeling and features multithreading and GPU acceleration, significantly improving computational efficiency for large-scale simulations. Its script-driven input method (via Python or text files) offers high flexibility, enabling precise control of simulation parameters. Additionally, Gprmax boasts cross-platform compatibility and is backed by an active developer community and comprehensive tutorial resources, providing a reliable numerical simulation tool for academic research and engineering practices.

When using Gprmax for FDTD forward modeling of HFEW, there are three main parameters to be set: 1) antenna parameters, including excitation source type, antenna spacing, antenna frequency, antenna type, output signal and recording time; 2) Geometric parameters of the model, including model size and mesh size; 3) The physical parameters of the model, that is, the physical parameters of the medium in the model area, including the relative dielectric constant, conductivity, relative permeability, etc [27].

3.2. The Goaf Model Design

Design a 3-layers geological model as shown in **Figure 2**, with a model size of 10m × 21m.The formation is homogeneous rather than heterogeneous [28]. The coal seam roof is both made of shale, the floor is made of sand, with a coal seam thickness of 5m and a roof and floor shale thickness of 3m. The goaf is located inside the coal seam, and the shape of the goaf is designed as a square (roadway goaf). The boreholes are located inside the coal seam; the borehole 1 is at the position cross the goaf center, while the borehole 2 is at the position 1m away from the coal seam

roof. The center of the goaf is 2m away from the coal seam floor. The model is shown in **Figure 2**.

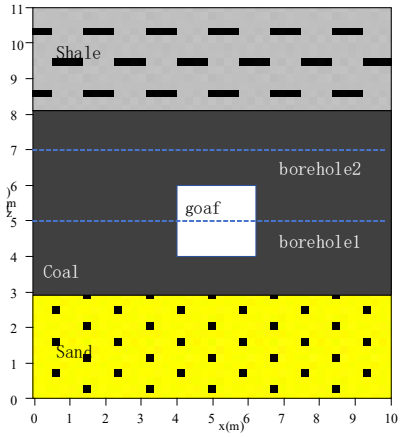

Figure 2. Schematic Diagram of Goaf Model (Goaf if Filled with Air).

So the relative dielectric constant of coal seams is 4, and the conductivity is 0.001 S/m. The relative dielectric constant of shale in coal seam roof is 8, conductivity is 0.01S/m random numbers. The relative dielectric constant of sand in coal seam floor is 6, conductivity is 0.1S/m. The goaf may be filled with water, or air. The physical properties of various media are shown in **Table 1**. We selected PML [29] for boundary conditions.

Table 1. The Parameters.

Parameter Type	Parameter Name	Value	Parameter Name	Value
Antenna Parameters	Center frequency (MHz)	100/200	Recording window (ns)	100
	Antenna spacing (m)	0.5	Incentive type	Ricker
	Antenna type	Dipole	output signal	Ez
Geometric Parameters	Area	10 m×11 m	Grid size (m)	0.01
	Coal seam thickness (m)	5	Thickness of top and bottom plate (m)	3
Physical Parameters	Coal seam conductivity (S/m)	0.001	Shale conductivity (S/m)	0.01
	Relative permeability of coal seam	4	Sand conductivity (S/m)	0.1
	Relative permeability of shale	8	Relative permeability of sand	6

3.3. The Goaf Simulation Characteristic

The goaf is filled with air. As shown in **Figure 3**, the results of detecting the goaf in borehole 1 using a 100 MHz HFEW are presented in **Figure 3(a)**, while those using a 200 MHz HFEW are shown in **Figure 3(b)**.

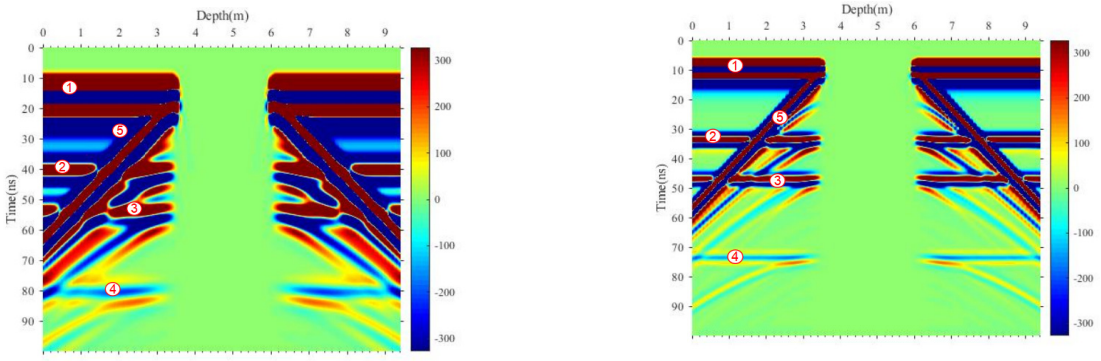

(a) **(b)**

Figure 3. Time Domain Profile of HFEW in Borehole 1. **(a)** HFEW is 100MHz in Borehole 1. **(b)** HFEW is 200MHz in Borehole 1.

In **Figure 3(a)** and **3(b)**, the in-phase axis labeled ① is the direct wave, Direct wave refers to electromagnetic waves emitted from a transmitting antenna, which do not propagate through geological layers but propagate directly through a borehole and are received by a receiving antenna.; the in-phase axis labeled ② is the reflection wave between the coal seam and the floor,the reflection wave between coal seam and floor refers to the electromagnetic waves emitted by the transmitting antenna, which enter the formation and reflected by the floor. The reflected waves are received by the receiving antenna; the in-phase axis labeled ③ is the reflection wave at the interface between the coal seam and the roof, the reflection wave between coal seam and roof refers to the electromagnetic waves emitted by the transmitting antenna, which enter the formation and reflected by the floor. The reflected waves are received by the receiving antenna; the in-phase axis labeled ④ is the multiple wave inside the coal seam,multiple waves between coal seams refer to the electromagnetic waves emitted by the transmitting antenna entering the formation, encountering the coal seam roof or floor to emit reflections, and the reflected waves encountering the coal seam floor or roof to emit reflections again, this reflected wave is received by the receiving antenna and belongs to a multiple wave between coal seams; the in-phase axis labeled ⑤ is the reflection wave generated in the goaf,the reflected wave in the goaf refers to the electromagnetic wave emitted by the transmitting antenna, which enters the formation and is reflected when encountering the goaf. After reflection, it is received by the receiving antenna. In **Figure 3(a)** and **3(b)**, the borehole passes through the goaf in the coal seam and affects the detection of the coal seam top and bottom interface. The direct wave, reflected wave at the top and bottom interface, and multiple wave phase axes are all truncated by the goaf, and the truncated area cannot display the top and bottom interface and multiple waves. In the actual detection process of the drilling radar, the presence of goaf around the borehole has an impact on the detection of the coal rock interface. The results of the 200 MHz center frequency detection in **Figure 3(b)** are clearer than those of the 100 MHz detection in **Figure 3(a)**.

As presented in **Figure 4**, the results of detecting the goaf in borehole 2 using 100 MHz HFEW are shown in **Figure 4(a)**, while those using 200 MHz HFEW are shown in **Figure 4(b)**.

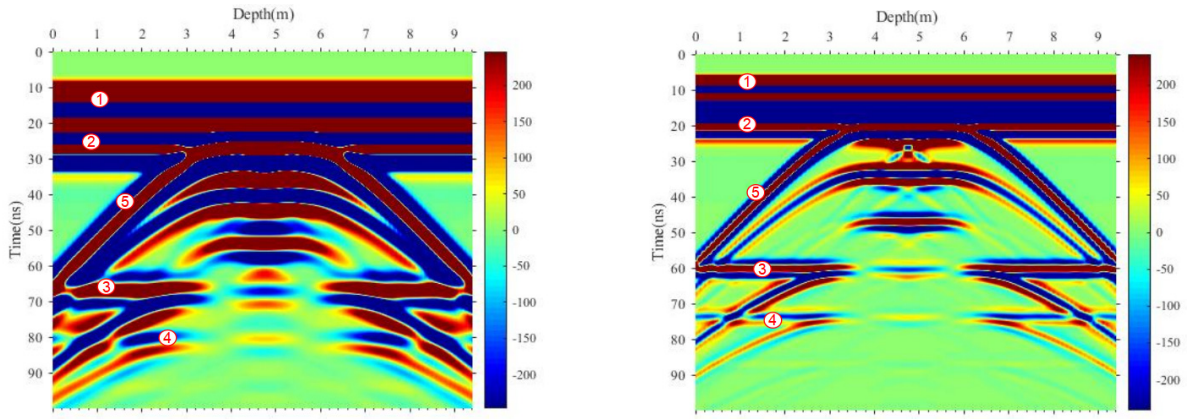

(a) **(b)**

Figure 4. Time Domain Profile of HFEW in Borehole 2. **(a)** HFEW is 100MHz in Borehole 2. **(b)** HFEW is 200MHz in Borehole 2.

In **Figure 4(a)** and **4(b)**, the meanings of each label ① – ⑤ are consistent with those in **Figure 3(a)**. In **Figure 4(a)** and **4(b)**, when there is a goaf in the coal seam and the borehole does not pass through the goaf, the goaf still has an impact on the detection of the top and bottom interface of the coal seam. The results of the 200 MHz center frequency detection in **Figure 4(b)** are clearer than the in-phase axis of the 100 MHz detection in **Figure 4(a)**.

In order to further analyze the response characteristics of different filling media in the goaf, the filling media in the goaf were changed to air, the upper half to air, and the lower half to water in the model shown in **Figure 2**. The response was obtained when the borehole distance was 1 m from the roof and the center frequency of the HFEW was 200 MHz, as shown in **Figure 5**.

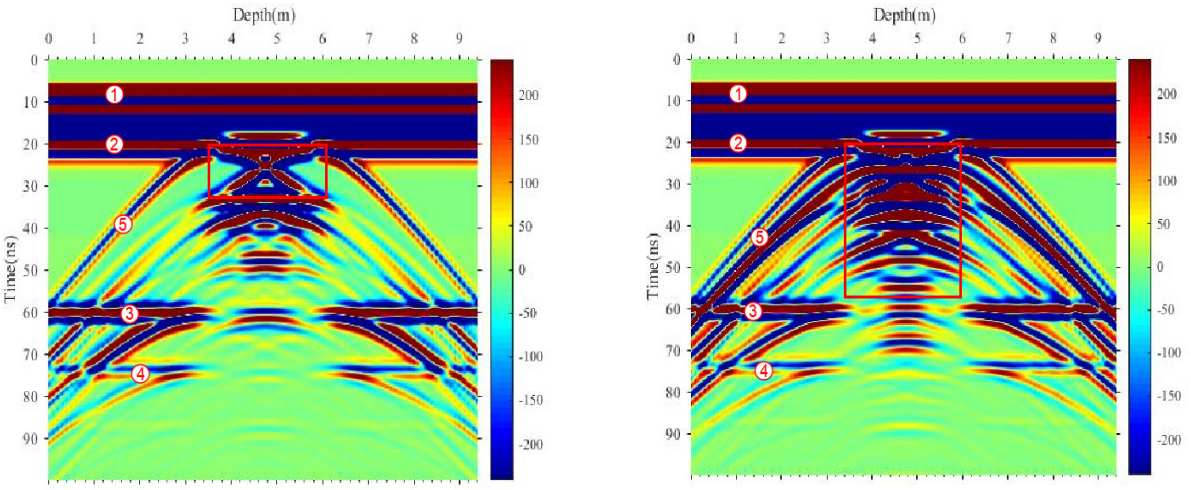

Figure 5. Time Domain Profile of Response to Changes in Fill Material in Goaf. **(a)** The Goaf is Filled with Air. **(b)** Half of the Goaf is Water and Half is Air.

The response characteristics of the borehole radar in the goaf filled with air in **Figure 5(a)** are opposite in phase to those in **Figure 4(a)** filled with water, and the boundary position of the goaf (indicated by the square in **Figure 5(a)**) is more obvious. The response characteristics of the borehole radar in the goaf filled with half air and half water in **Figure 4(b)** are more complex compared to those filled with air or water, and the hyperbolic axis marked with ⑤ is more complex. At the same time, new reflection axes will be superimposed at the interface between water and air. In practical applications, the filling material in goaf can be analyzed by examining the characteristics of the same phase axis.

4. Application

A large open-pit mine in Inner Mongolia, China, with a long history of coal extraction, faces significant geohazards due to numerous undocumented small goaf zones within its 7-meter-thick coal seams. These hidden voids, posing critical safety risks, render traditional surface-based exploration methods ineffective. To address this challenge, directional long boreholes (230-meter depth) were constructed along the coal seam from the mining platform. A 100 MHz high-frequency electromagnetic wave (HFEW) system was deployed to detect goaf anomalies within the boreholes. The instrument is shown in **Figure 6**; the parameters of the instrument is list in **Table 2**. The instrument is sent into the hole through a drilling rig for detection. The instrument performs real-time detection inside the hole, and the detection data is stored in the instrument. Depth markings are made outside the hole. After the measurement is completed, the instrument is lifted to the hole mouth, and the data measured inside the instrument is exported to the hole mouth equipment for matching with the depth. The assembly of the instrument during on-site operation is shown in **Figure 7**. The raw data profile from this investigation is shown in **Figure 8**.

Figure 6. HFEW Instrument.

Table 2. The Parameters of the Instrument.

Parameter Names	Values
Center frequency	100MHz
Antenna type	Dipole antenna
Diameter	50mm
Length	2.7m
Scans/second	10
Bits/sample	16
Samples/scan	512 or 1024 or 2048
Stacking	32
A/D	24
Gain range	−12dB ~ 128dB

Figure 7. On Site Assembly Diagram of the Instrument.

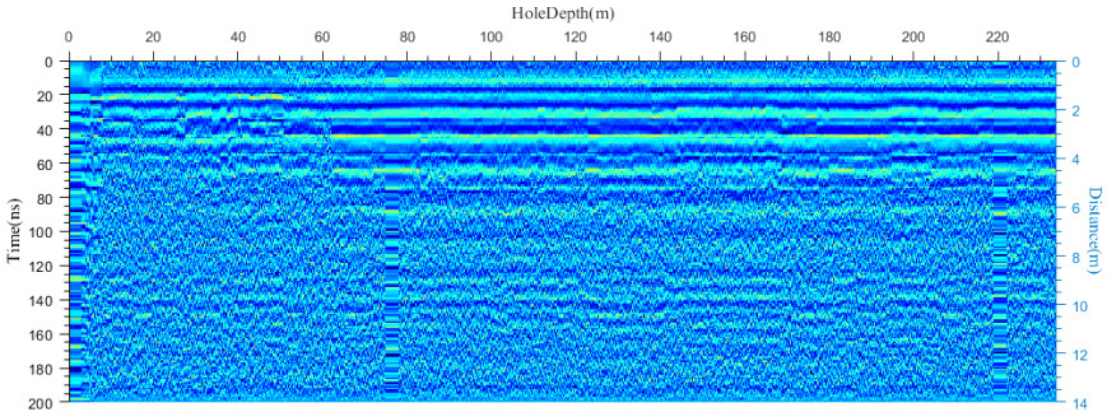

Figure 8. HFEW Raw Data Profile of Open-Pit Mine Along Coal Seam Boreholeg Exploration Goaf.

As illustrated in **Figure 8**, direct identification of goaf boundaries from unprocessed data remains ambiguous, necessitating advanced signal analysis. The data processing workflow comprises the following key steps:

1) Data Pre-processing and Analysis. Perform pre-processing and analysis of the data to estimate the signal-to-noise ratio (SNR) level and identify the primary frequency bands of effective energy. This provides a basis for parameter selection and evaluation of processing quality in subsequent steps.

2) Estimation of Vector Included Angle Between Adjacent Traces. Improve the accuracy of vector included angle estimation by applying lateral interpolation to adjacent borehole radar traces.

3) Multi-Directional Dip Scanning to Derive the "Unit Correlation Vector "Conventionally, the amplitude signals of direct wave arrivals are extracted laterally, and the "unit correlation vector" is obtained by vector summation of

multiple adjacent signals. To address potential misalignment of direct wave arrivals, a small angular search range is defined. Amplitude signals are extracted along the dip direction to ensure the derived "unit correlation vector" aligns as closely as possible with the effective signal direction.

4) Signal-to-Noise Separation. Select appropriate parameters to perform true amplitude extraction for separating signals from noise.

5) Vector Angle Smoothing Constraint. Apply smoothing constraints to the vector angles between adjacent traces in the true amplitude gather.

6) Quality Control. Evaluate whether the extracted signals are compromised or degraded during processing.

7) Resampling. Resample the processed data to match the original trace's sampling rate, outputting the noise-suppressed dataset.

After processing with the method, it is shown in **Figure 9**.

After processing method described in this article, **Figure 9** shows obvious hyperbolic structural features at a depth of about 20 meters and a distance of about 3 meters from the borehole. The phase is consistent with that of the direct wave, which is a typical structural response feature of waterless goaf; After the area was stripped during mining, a waterless goaf approximately 3 meters in diameter was revealed at this location, as illustrated in **Figure 10**, confirming the results presented in **Figure 9**.

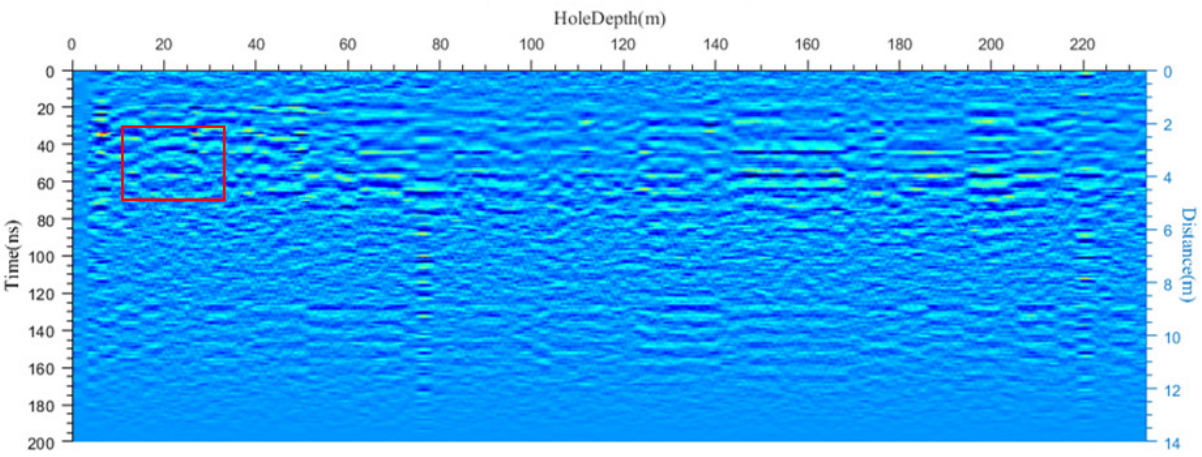

Figure 9. HFEW Data Profile After Processing.

Figure 10. Mining Exposure Goaf Photo.

5. Conclusions

This study establishes a numerical model for goaf detection in near-horizontal coal mine boreholes using high-frequency electromagnetic waves.

The results demonstrate that when HFEW is deployed in parallel horizontal boreholes, the goaf exhibits distinct hyperbolic reflection phase-axis signatures.

Notably, the phase-axis characteristics vary depending on the fluid type (e.g., air, water) and saturation state (saturated vs. unsaturated) within the goaf. When the goaf is filled with air, the phase of the reflected wave in the goaf is the same as that of the direct wave, and multiple waves are generated inside the goaf; When there is water in the goaf, the phase of the reflected wave in the goaf is opposite to that of the direct wave; When the interior of the goaf is divided into water and air, more multiple waves will be generated.

These differential phase responses enable High-Frequency Electromagnetic Wave to not only pinpoint goaf locations but also characterize fluid properties within the voids. Field validation in operational coal mines confirms the method's efficacy, underscoring its potential for enhancing goaf detection accuracy and safety in complex mining environments.

This method utilizes boreholes in coal mines for advanced detection, and only requires the HFEW equipment to be inserted into the hole. The entire operation process is simple, the required time is short, and the cost is not high, making it more suitable for promotion and application. Field tests in Inner Mongolia demonstrated the system's effectiveness, achieving a 15–20-meter radial detection radius per borehole (20 times greater than traditional logging) and 40% faster scanning efficiency compared to seismic methods.

Funding

This work received no external funding.

Institutional Review Board Statement

Not applicable

Informed Consent Statement

Not applicable.

Data Availability Statement

The data that support the findings of this study are derived from actual mine data, which cannot be made publicly available due to privacy and confidentiality restrictions. The data contain sensitive information about the mining operations and related parties that could potentially compromise the security and competitive position of the mining company involved. Access to such data is subject to strict regulations and agreements that prevent us from sharing the raw data outside of the research context.

Acknowledgments

I would like to express my sincere gratitude to UCHN Energy Investment Group SHEN DONG COAL Geological Survey Company for their unwavering support throughout the duration of this research project. Their contributions have been instrumental in providing the necessary resources and environment that facilitated the successful completion of my work.

Conflicts of Interest

The author declares no conflict of interest.

References

[1] Yang, Y., 2023. Three dimensional forward and backward modeling research and application of fre-quency domain controllable source electromagnetic method in coal mine goaf [PhD's Thesis in Chinese]. Guilin University of Technology: Guilin, China. DOI: https://doi.org/ 10.27050/d.cnki.gglgc.2023.000003

[2] Liu, W., 2023. Application research of comprehensive geophysical exploration technology in coal mine goaf detection. Energy and Energy Conservation [in Chinese]. Energy and Energy Conservation. 23(5), 193–195+211. DOI: https://doi.org/DOI:10.16643/j.cnki.14-1360/td.2023.05.056

[3] Liu, Y., 2007. Seismic exploration methods on goaf [in Chinese]. Science and Technology Consulting Herald. 27(4), 100–101. DOI: https://doi.org/10.16660/j.cnki.1674-098x.2007.17.072

[4] Zhang, X., Huang, J., Song, L., et al., 2010. Appli-

cation of ground penetrating radar (GPR) exploration in Karst mountain areas. Proceedings of the 13th International Conference on Ground Penetrating Radar; 21–25 June 2010; Lecce, Italy. pp. 1–4.

[5] Investigation report on the "4.16" roof collapse accident at Xieqiao Coal Mine of Huainan Mining (Group) Co., Ltd. Available from: https://www.mkaq.org/html/2018/12/17/469111.shtml (cited February 25 2025).

[6] Lin, J., Xue, G., Li, X., 2021. Technological innovation of semi-airborne electromagnetic detection method [in Chinese]. Chinese Journal of Geophysics [in Chinese]. 64(9), 2995–3004. DOI: https://doi.org/10.6038/cjg2021P0409

[7] Qi C.Y., 2014. Research on Fire Detection and Fire Prevention Technology in the goaf of Anjialing Open pit Mine [Master's thesis]. Liaoning University of Engineering and Technology: Fuxin City, China.

[8] Jiang J.,Wang J.,Zhang D., et al., 2021. Application of high-precision magnetic survey in the detection of magnetic veins in a mine in North China [in Chinese]. China Coal Geology. 33(10), 175.

[9] Fan, T., Li, H., Guo, J., et al., 2020. Application of borehole transient electromagnetic pseudo seismic inversion method in fine exploration of goaf in open-pit coal mines. Journal of Earth Science and Environment. 42(6), 759–766.

[10] Jun, Z., 2020. The high-resolution transient electromagnetic detection technology for ultra-shallow layer in coal mine. Coal Geology and Exploration. 48(4), 219–225. DOI: https://doi.org/10.3969/j.issn.1001-1986.2020.04.030

[11] Hou, Y., Guo, J., Si, Y., et al., 2021. Research on three-component response of ground-airborne TEM considering emission current waveform. Coal Geology and Exploration. 49(5), 27. DOI: https://doi.org/10.3969/j.issn.1001-1986.2021.05.026

[12] Li, Z., Yang, H., Yue, J., et al., 2022. Conical source transient electromagnetic response characteristics with overburden based on Occam constrained inversion. Coal Geology and Exploration. 50(6), 175–183. DOI: https://doi.org/10.12363/issn.1001-1986.22.01.0023

[13] Wang, S., Yang, C., 2015. Selection of detection methods for goaf. Coal Technology. 34(09), 225–228. DOI: https://doi.org/10.13301/j.cnki.ct.2015.09.085

[14] Xin, S.H., Song, R.C., Yang J.J., et al., 2008. Application of High-density Electrical Method in Coalmine Goaf Surveying. Coal Geology of China. (01), 59–61.

[15] Mo, L., 2019. Research on Comprehensive Geophysical Exploration Method for Coal Mine Goaf in LZC Area, Inner Mongolia [Master's Thesis]. China University of Mining and Technology: Xuzhou, China.

[16] Xue G.Q,Pan D.M., Yu J.T., 2018. Review the applications of geophysical methods for mapping coalmine voids [in Chinese]. Progress in Geophysics. 33(5), 2187–2192. DOI: https://doi.org/10.6038/pg2018BB0294

[17] Chen Y.L., Tang J., 2022. Logging Evaluation of Fracture-cavity Systems in Carbonate Reservoirs of Tuofutai Area, Tarim Basin, Xinjiang. Chinese Journal of Engineering Geophysics. 19(5), 689–698. DOI: https://doi.org/10.3969/j.issn.1672-7940.2022.05.015

[18] Cao Z.J.,Tang K.Y., 2019. Application of comprehensive method to the prospecting project and the effect in the Zhuxianzhuang coal mining settlement area, Anhui province. Contributions to Geology and Mineral Resources Research. 34(3), 478–484. DOI: https://doi.org/10.6053/j.issn.1001-1412.2019.03.019

[19] Cheng, J., Hu, K., Wang, Y., et al., 2004. Research on Ground Penetrating Radar Detection of Underground Mining Areas[J]. Geotechnical Mechanics. 25(S1), 79–82.

[20] Rumpf, M., Tronicke, J., 2014. Predicting 2D geotechnical parameter fields in near-surface sedi-mentary environments. Journal of Applied Geophysics. 101, 95–107. DOI: https://doi.org/10.1016/j.jappgeo.2013.12.002

[21] Hu, F., Wu, M., Xu, D., et al., 2018. Using electromagnetic wave CT technology for perspective imaging in karst areas. CT Theory and Application Research. 27(02), 205–212. DOI: https://doi.org/10.15953/j.1004-4140.2018.27.02.09

[22] Singh, K.K.K., 2015. Borehole radar for delineation of unapproachable underground coal-mine galleries below Grand Chord railway lines. Current Science. 109(9), 1722–1727.

[23] Liu, S., Zeng, Z., Sato, M., 2005. Subsurface water-filled fracture detection by borehole radar: a case history. Proceedings of the 2005 IEEE International Geoscience and Remote Sensing Symposium; 25–29 July 2005; Seoul, Korea. pp. 360–363.

[24] Zeng, Z., Li, S., Feng, X., 2010. Principle and application of ground penetrating radar. Electronic Industry Press: Beijing, China.

[25] Warren, D.C., Giannopoulos, D.A., Giannakis, D.I., et al., 2016. GprMax: Open source software to simulate electromagnetic wave propagation for ground penetrating radar. Computer Physics Communications. 209, 163–170. DOI: https://doi.org/10.1016/j.cpc.2016.08.020

[26] Warren, C., Giannopoulos, A., Gray, A., et al., 2019.

A CUDA-based GPU engine for gprMax: open source FDTD electromagnetic simulation software. Computer Physics Communications. 237, 208–218. DOI: https://doi.org/10.1016/j.cpc.2018.11.007

[27] Zhong, S., 2008. Key issues of dynamic exploration survey based on the borehole radar and digital imaging [PhD thesis]. Wuhan Institute of Rock and Soil Mechanics: Wuhan, China.

[28] Li, J., 2014. Random equivalent medium ground penetrating radar detection technology and parameter inversion [Ph.D. thesis]. Jilin University: Changchun, China. Available from: CNKI (cited 16 November 2024).

[29] Giannopoulos, A., 2008. An improved new implementation of complex frequency shifted PML for the FDTD method. IEEE Transactions on Antennas and Propagation. 56(9), 2817–2825. DOI: https://doi.org/10.1109/TAP.2008.928791